Acta Applicandae Mathematicae (2024) 194:11
https://doi.org/10.1007/s10440-024-00700-y

Reduced Order Model Based Nonlinear Waveform Inversion for the 1D Helmholtz Equation

Andreas Tataris[1] · **Tristan van Leeuwen**[2,3]

Received: 7 September 2023 / Accepted: 30 October 2024

Abstract
We study a reduced order model (ROM) based waveform inversion method applied to a Helmholtz problem with impedance boundary conditions and variable refractive index. The first goal of this paper is to obtain relations that allow the reconstruction of the Galerkin projection of the continuous problem onto the space spanned by solutions of the Helmholtz equation. The second goal is to study the introduced nonlinear optimization method based on the ROM aimed to estimate the refractive index from reflection and transmission data. Finally we compare numerically our method to the conventional least squares inversion based on minimizing the distance between modelled to measured data.

Keywords Reduced order models · Nonlinear inversion · Helmholtz equation · Full waveform inversion

1 Introduction

Reduced order model techniques have been studied for a long time in the context of solving boundary value problems numerically. The main difference between conventional finite element methods and the reduced order model (ROM) approach is that in the latter, one approximates the solution of the problem in a finite-dimensional subspace spanned by solutions of the PDE itself (i.e., solutions for different wavenumbers in case of the Helmholtz equation). The advantage of using the ROM method for solving forward boundary value problems is the rapid convergence of the approximates to the true solution of the problem. We refer the interested reader to [1–4] and the references therein for more information on the subject.

Recently, reduced order model techniques have received attention and have been applied to Neumann inverse boundary value problems for estimating coefficients of diffusion type

✉ A. Tataris
a.tataris@tudelft.nl

T. van Leeuwen
t.vanleeuwen@uu.nl

1 Delft Institute of Applied Mathematics, Delft University of Technology, Delft, The Netherlands

2 Mathematical Institute, Utrecht University, Utrecht, The Netherlands

3 Computational Imaging, Centrum Wiskunde & Informatica, Amsterdam, The Netherlands

Published online: 13 November 2024

elliptic partial differential equations, see [5] [6]. In short, in the cited papers, the authors consider boundary traces of solutions of the diffusion equation that correspond to a discrete set of spectral parameters. Using these measurements they reconstruct the so-called ROM matrices (often called as ROM projections), which describe the restriction of the differential operator on the finite dimensional space spanned by solutions of the forward problem. Using the Lanczos algorithm (see [7]) and the ROM matrices as input, it is possible to linearise the inverse problem by obtaining an estimate of the state using some knowledge of a reference coefficient. Subsequently the unknown coefficient can be estimated by solving an integral equation. Roughly speaking, the use of the ROM method to obtain a linearised solution of the inverse problem can be thought as a discrete analog of the classical Gelfand-Levitan-Marchenko approach, see [8–12].

The approach that we take in this paper was inspired by similar works developed for time-domain wave propagation with Dirichlet boundary conditions, see [13, 14] and [15]. For practical applications, however, impedance boundary conditions are of great interest since they are equivalent to the Sommerfeld radiation condition in 1D (and an approximation of the radiation condition in two and three dimensions). Also, in this paper we present a method that requires the so-called ROM projections as input for optimization as opposed to the works cited above. In particular, in the above works, the authors apply the nonlinear Lanczos transform on the ROM projections, and they use the transformed matrices as input. Despite possible variations of a Lanczos based ROM waveform inversion that could be defined for the Helmholtz impedance problem, we would like to investigate a ROM based optimization method that avoids the use of the Lanczos method altogether. One reason to avoid using the Lanczos method is the induced instability, as we saw in [16]. Therefore, in this paper we explore how a ROM based nonlinear inversion approach can be applied to the Helmholtz framework, by studying the one dimensional case and using the reconstructed ROM projections as input for optimization. The motivation behind studying the ROM method within an optimization framework are the promising results that have been observed in the time-domain setting. Also, as we shall see in detail, in the case where we consider impedance boundary conditions, the stiffness and mass (ROM) matrices do not depend linearly on the data. Thus we expect different convexity properties for misfit functionals based on the ROM approach compared with functionals based on the conventional so-called full waveform inversion (FWI) approach based on minimizing the distance between modelled to measured data. In comparison to our previous work ([16]) where we studied *Linearization type methods* using the Lanczos method and data assimilation to solve the inverse problem for the Schödinger case, here, in the Helmholtz case, we employ nonlinear optimization and we avoid completely the involvement of the Lanczos method to solve the inverse problem.

Our main contributions in this paper include the introduction of our nonlinear inversion method based on ROMs in the frequency domain, and the study of its well posedness in an infinite dimensional framework. In particular, we solve the inverse scattering problem using the ROM method in an optimization framework without using Lanczos (or any other) orthogonalization for the ROM. We also compare our method to the conventional full waveform inversion method in terms of the convexity of the misfit functionals, and how accurately each method reconstructs a coefficient (refractive index of Helmholtz operator) using both noiseless and noisy measurements.

The paper is organized as follows. We start with Sect. 2 where we present a couple of well-posedness results regarding the forward problem. In Sect. 3 we present the main results. In particular we explain how to recover the ROM matrices using double sided data. We also study the well-posedness of the associated nonlinear variational inverse problem

and we present the optimality condition. We continue with Sect. 4 where we present several numerical experiments of our ROM based FWI method and we conclude the paper with a discussion section.

2 Preliminaries

In this section we provide some preliminaries and well known results needed for later. Our forward problem is to find a weak solution $u \in H^1(0,1)$ such that

$$\Big(-\frac{d^2}{dx^2} - k^2 m\Big)u(k) = 0,\ x \in (0,1) \tag{1}$$

$$u'(k) + \imath k u(k) = 1,\ x = 0 \tag{2}$$

$$u'(k) - \imath k u(k) = 0,\ x = 1. \tag{3}$$

We assume that $k > 0$ and that the coefficient m, is an element of the admissible set

$$\mathbb{K}_{ad} := \{m \in H^1((0,1);[1,\infty)),\ m(0) = m(1) = 1\}. \tag{4}$$

In a variational framework, the above differential equation becomes,

$$(u'(k), \psi') - k^2(mu(k), \psi) - \imath k\{u(k)|_{x=1}\overline{\psi(1)} + u(k)|_{x=0}\overline{\psi(0)}\} = -\overline{\psi(0)}, \tag{5}$$

$$\forall \psi \in H^1(0,1).$$

Here, $(\cdot,\cdot)$ denotes the L^2-inner product. We now present some known results about the forward problem. Well-posedness of the forward problem can be shown either using the Lax-Milgram theory, see for example [17] or [18], or using the equivalent Lippmann-Schwinger equation of the direct scattering problem. We denote the anti-dual of H^1 as $\overline{H^{1'}}$ and the brackets $\langle\cdot,\cdot\rangle$ denote duality.

Proposition 1 *Given $k > 0$, there exist a unique solution $u(k,m) \in H^1(0,1)$ that satisfies the state equation (1)-(3).*

Proof A more detailed sketch of the proof can be found in the appendix, and for full details we refer to [10, 18]. In short, the forward problem can be reduced to the following linear problem, of finding $u \in H^1(0,1)$:

$$\Phi\mathcal{T}(\mathcal{I} + k^2\mathcal{A})u = -\delta_0,\ \overline{H^1(0,1)}', \tag{6}$$

where Φ is the linear Riesz isomorphism, $\mathcal{T}$ is defined through the form

$$a_1(u,v) = \int_0^1 u'\overline{v'}dx - ik\{(u\overline{v})|_{x=0} + (u\overline{v})|_{x=1}\},\ u, v \in H^1, \tag{7}$$

such that

$$a_1(u,v) = (\mathcal{T}u, v)_{H^1},\ u, v \in H^1, \tag{8}$$

where δ_0 is the Dirac measure ("delta" distribution) supported on 0. We define $\mathcal{V}$ such that

$$\langle \mathcal{V}u, v\rangle = a_2(u, v) = \int_0^1 mu\overline{v}dx,\ u, v \in H^1, \tag{9}$$

and $\mathcal{A} = \mathcal{T}^{-1}\Phi^{-1}\mathcal{V}i_{H^1\to L^2}$, where $i_{H^1\to L^2}$ is the compact imbedding operator of $H^1(0, 1)$ to $L^2(0, 1)$. □

Corollary 2 *The traces*

$$f(\lambda) = u(\sqrt{\lambda})|_{x=0},\ g(\lambda) = u(\sqrt{\lambda})|_{x=1},\ \lambda > 0 \tag{10}$$

are well defined.

We assume to have measurements of the solutions for a discrete set of wavenumbers,

$$\mathbb{W} = \{k_i : i = 1, \ldots, N\},$$

of the form

$$f(k^2) = u(k)|_{x=0},\ g(k^2) = u(k)|_{x=1}. \tag{11}$$

From the data we reconstruct the ROM projection of the forward scattering problem onto the finite dimensional space

$$\mathbb{X}_N = \text{span}\{u_i : i = 1, \ldots N\}, \tag{12}$$

with $u_i = u(k_i)$. As we shall see in detail, this projection yields three matrices, the stiffness, the mass and the boundary matrix, S, M, B respectively.

3 Main Results

In this section we present our main results. We start with describing how to recover the so-called ROM matrices from double-sided data. We then continue with the study of our ROM based nonlinear inversion method.

3.1 ROM Matrices Construction Using Two-Sided Data

In this paragraph we describe the passage from boundary measurements to the ROM projections of the forward problem. We can express (5) equivalently as

$$(\mathcal{S} - k^2\mathcal{M}(m) - \imath k\mathcal{B})u = -\delta_0, \tag{13}$$

as an $\overline{H^1(0, 1)}'$ relation. For example

$$\mathcal{S} : H^1(0, 1) \to \overline{H^1(0, 1)}' \tag{14}$$

acts as follows

$$\langle \mathcal{S}y, \phi\rangle = (y', \phi'). \tag{15}$$

Similarly, we define $\mathcal{M}, \mathcal{B}$.

Remark 1 For the sake of completeness, it is useful to connect $\mathcal{S}, \mathcal{M}, \mathcal{B}$ with the operators used in the proof of proposition 1. We get

$$\langle(\mathcal{S} - k^2\mathcal{M}(m) - \imath k\mathcal{B})u, v\rangle = -\langle\delta_0, v\rangle,\ \forall v \in H^1, \tag{16}$$

or

$$\langle(\mathcal{S} - k^2\mathcal{M}(m) - \imath k\mathcal{B})u, v\rangle = a_1(u, v) - k^2 a_2(u, v) = (\mathcal{T}(I + k^2\mathcal{A})u, v)_{H^1} = \tag{17}$$

$$\langle\Phi\mathcal{T}(I + k^2\mathcal{A})u, v\rangle,\ \forall v \in H^1. \tag{18}$$

Therefore

$$\mathcal{S} - k^2\mathcal{M}(m) - \imath k\mathcal{B} = \Phi\mathcal{T}(\mathcal{I} + k^2\mathcal{A}) \tag{19}$$

We now consider relation (13) on $\mathbb{X}_N$ which is spanned by exact solutions that correspond to different wavenumbers, as explained in Sect. 2. We first observe that we can restrict $\mathcal{S}$ on $\mathbb{X}_N$ such that

$$\langle\mathcal{S}|_{\mathbb{X}_n}u, \phi\rangle = \langle\mathcal{S}u, \phi\rangle, u \in \mathbb{X}_N, \phi \in H^1(0, 1). \tag{20}$$

and subsequently the elements

$$\langle\mathcal{S}|_{\mathbb{X}_N}u, \phi\rangle = \langle\mathcal{S}u, \phi\rangle, u \in \mathbb{X}_N, \phi \in \mathbb{X}_N. \tag{21}$$

This way, we define the stiffness matrix, $S \in \mathbb{C}^{N\times N}$ with entries

$$S_{ij} = \langle\mathcal{S}u_i, u_j\rangle = (u_i', u_j'),\ i, j \in \{1, \dots N\}. \tag{22}$$

Similarly, we define the mass matrix

$$M_{ij} = (mu_i, u_j),\ i, j \in \{1, \dots N\}, \tag{23}$$

and the matrix containing the boundary responses

$$B_{ij} = g_i\overline{g_j} + f_i\overline{f_j},\ i, j \in \{1, \dots N\}. \tag{24}$$

The main characteristic making this approach useful for solving the inverse problem, is that the ROM matrices can be computed directly from the data. From now on we denote

$$f_i = f(k_i^2),\ i = 1, \dots, N,$$

and

$$g_i = g(k_i^2),\ i = 1, \dots, N.$$

Lemma 3 *The ROM system matrices S, M are given in terms of the boundary data*

$$M_{ij} = -\frac{\overline{f_j} - f_i}{k_j^2 - k_i^2} + \imath\frac{g_i\overline{g_j} + f_i\overline{f_j}}{k_j - k_i},\ i \neq j, \tag{25}$$

$$M_{ii} = \Big\{ - Re(f')(\lambda) + 2\sqrt{\lambda}\Big(\overline{g(\lambda)}g'(\lambda) + \overline{f(\lambda)}f'(\lambda)\Big)\Big|_{\lambda=k_i^2}$$

$$S_{ij} = -\frac{k_j^2\overline{f_j} - k_i^2 f_i}{k_j^2 - k_i^2} + \iota(k_j^2 k_i + k_i^2 k_j)\frac{g_i\overline{g}_j + f_i\overline{f}_j}{k_j^2 - k_i^2},\ i \neq j, \tag{26}$$

$$S_{ii} = \left\{(-\lambda Re(f)'(\lambda) - Re(f)(\lambda)) + 2\lambda^{3/2} Im\left(\overline{g(\lambda)}g'(\lambda) + \overline{f(\lambda)}f'(\lambda)\right)\right\}\Big|_{\lambda=k_i^2} \tag{27}$$

$i, j = 1, \ldots, N$.

Proof The proof can be found in the appendix A.2. □

Remark 2 Observe that for our scattering framework that involves impedance boundary conditions, having measurements at both sides of the interval is crucial to reconstruct the ROM matrices (similarly as in our study of the Schrödinger case [16]). In comparison to the current setting, in the Neumann (or analogously Dirichlet) case (see [5]), having double sided data is not necessary to reconstruct the mass and the stiffness matrices. This is because no boundary terms or integrals appear in the weak form of the differential equation (contrary to the scattering case that we study here). Using double sided data and one source in the context of the ROM based inversion has been also considered in [19].

Remark 3 Observe that in $\mathbb{R}^{2,3}$, similar relations as in the above lemma will hold true. In particular, in the multidimensional Helmholtz impedance boundary value problem, we need to have knowledge of the wavefields throughout the entire boundary of our domain in order to reconstruct the ROM matrices.

3.2 Solving the Inverse Problem with Nonlinear Optimization

In this paragraph we study a nonlinear inversion method based on the ROM approach. As we discussed in the introduction, our proposed optimization method serves as an option for using the ROM apparatus to the Helmholtz framework. In the case of the Schrödinger equation for example, a linearization type technique based on the Lanczos method could be also used [16]. The Lanczos method has been also combined with nonlinear optimization in the Dirichlet and Neumann setting. In particular, in the Dirichlet case, see, [13, 15], the input for the optimization is the tridiagonal matrix that the Lanczos orthogonalisation method returns using the ROM projections as input.

Is important to note that within the Helmholtz framework, we would wish to avoid using the Lancszos method completely. Unlike orthogonalization with respect to the usual L^2-inner product, see [5, 16], orthogonalizing with respect to an inner product influenced by the unknown, m, might not yield snapshots that depend weakly on the medium. That means that the orthogonalized snapshots can potentially include multiple scattering behaviours inside the volume of the domain.

In the Helmholtz setting of this paper we consider an optimization alternative for solving the inverse problem that requires the stiffness matrix only as input. Despite possible variations of a ROM based optimization combined with the Lanczos method that can be defined particularly for the Helmholtz impedance case, one should be aware of the possible issues regarding the stability of the Lanczos algorithm as noted in [16]. In any case, with our work we want to investigate a ROM based optimization method that avoids the Lanczos method altogether.

Now, after acquiring the ROM matrix, $S = S^{obs.}$, we set up the following nonlinear optimization problem of estimating the refractive index m, using the stiffness matrix $S^{obs.}$ as

input:

$$\min\{\phi(m) : m \in \mathbb{K}_{ad}\} \tag{28}$$

with

$$\phi(m) := \frac{1}{2}\|S^{obs.} - S(m)\|_F^2 + \frac{\varepsilon}{2}\|m\|_{H^1(0,1)}^2, \text{ for some } \varepsilon > 0. \tag{29}$$

$S(m)$ is given according to relation (22) for a given m, and $\|\cdot\|_F$ is the Frobenius norm (i.e. we try to estimate m by matching modelled $S(m)$ with reconstructed $S^{obs.}$). We refer to relation (4) for the definition of the admissible set $\mathbb{K}_{ad}$. The special form of the functional that implicitly defines ϕ, let J, (product of wavefields in the computation of the modelled stiffness) makes showing existence of minimizers interesting. In particular since J is a sum of both weakly lower semicontinuous and not weakly lower semicontinuous functionals there is no guarantee on the behaviour of ϕ in terms of weak lower semicontinuity.

3.2.1 Existence of Minimizers

There are many ways of showing existence of minimizers in optimal control problems, see e.g. [20]. Here, the form that the elements of our modeled data have (elements of S are L^2 inner-products of the derivatives of the states) are not standard and create challenges in proving existence of solutions for the inverse problem. To be specific, the functional that implicitly defines ϕ through the reduced formulation includes non-weakly lower semicontinuous terms. In this framework, it is convenient to analyse the coefficient to state map $m \mapsto u(m)$ for showing well-posedness for the optimization problem. Showing "smoothness" of the coefficient to state map has been shown formally in the $\mathbb{R}^{2,3}$ scattering problem, see [21]. We work similarly here. Also, with ∂_1, ∂_2 we denote the partial Fréchet derivatives with respect to the first and second variables of a function respectively.

We consider the function $F : C([0,1]; (0,\infty)) \times H^1(0,1) \to \overline{H^1(0,1)}'$ given by

$$F(m,u) = (\mathcal{S} - k^2\mathcal{M}(m) - \imath k\mathcal{B})u + \delta_0, \ (m,u) \in C([0,1]; (0,\infty)) \times H^1(0,1). \tag{30}$$

Using the implicit function theorem applied on F, we obtain that a wavefield u is a smooth function of the coefficient m as stated below.

Lemma 4 *Given $k > 0$, the map $C([0,1]; (0,\infty)) \ni m \to u(k,m) \in H^1(0,1)$ is continuous and Fréchet differentiable.*

All details on the above lemma are given in the appendix A.3. Now, we are ready show existence of minimizers for the variational inverse problem of our study.

Remark 4 As we shall see in the proof of the following theorem, it is convenient to study the smoothness of u as a function of $m \in C[0,1]$ since we will make a passage from H^1-weakly convergent sequence of coefficients to $C[0,1]$-strongly convergent sequences.

Theorem 5 *The misfit functional ϕ as defined in relation (29) obtains minimizers on the admissible class $\mathbb{K}_{ad} = \{m \in H^1((0,1); [1,\infty)),\ m(0) = m(1) = 1\}$.*

Proof We denote

$$\phi(m) = \frac{1}{2}\sum_{i,j=1}^{N}\left\{|S_{ij}(m) - S_{ij}^{obs.}|^2\right\} + \frac{\varepsilon}{2}\|m\|^2_{H^1(0,1)} =$$

$$\frac{1}{2}\sum_{i,j=1}^{N}\phi_{ij}(m) + \frac{\varepsilon}{2}\|m\|^2_{H^1(0,1)}, m \in \mathbb{K}_{ad}. \tag{31}$$

Let $(i, j) \in \{1, \ldots, N\}^2$. Since $\phi \geq 0$ for all $m \in \mathbb{K}_{ad}$, there exists $\mu > 0$ such that

$$\mu = \inf_{m\in\mathbb{K}_{ad}} \phi_{ij}(m). \tag{32}$$

Therefore there is a sequence

$$(\phi(m_\nu))_{\nu\in\mathbb{N}} \subset \{\phi(m) : m \in \mathbb{K}_{ad}\} \tag{33}$$

such that

$$\phi(m_\nu) \to \mu, \ \nu \to \infty. \tag{34}$$

Since we use a regularization parameter, and since $\{\phi(m_\nu)\}_\nu$ is included in a ball, it follows that the sequence $(m_\nu)_{\nu\in\mathbb{N}} \subset \mathbb{K}_{ad}$ is bounded. Therefore, there is a subsequence $(m_\nu)_{\nu\in N_1} \subset (m_\nu)_{\nu\in\mathbb{N}}$ that has a weak limit, let $\widehat{m}$, in $\sigma(H^1, H^{1'})$. Symbolically

$$m_\nu \rightharpoonup \widehat{m} \ \text{ in } \sigma(H^1((0,1),\mathbb{R}), H^1((0,1),\mathbb{R})'). \tag{35}$$

$\widehat{m}$ is included in $\mathbb{K}_{ad}$ since the set is closed and convex. Due to the Sobolev's compact embedding we also obtain that

$$m_\nu \to \widehat{m} \ \text{ in } C([0,1];\mathbb{R}). \tag{36}$$

Since $u(k, \cdot)$ is continuous as a function of m, we obtain for every $i, j = 1, \ldots, N$ that

$$u(k_i, m_\nu) \to u(k_i, \widehat{m}), \ \text{ in } H^1(0,1) \tag{37}$$

and

$$u(k_j, m_\nu) \to u(k_j, \widehat{m}), \ \text{ in } H^1(0,1), \tag{38}$$

as $\nu \to \infty$. Since $\frac{d}{dx} : H^1(0,1) \to L^2(0,1)$ is bounded, we obtain that

$$\frac{du(k_i, m_\nu)}{dx} \to \frac{du(k_i, \widehat{m})}{dx}, \ \text{ in } L^2(0,1) \tag{39}$$

and

$$\frac{du(k_j, m_\nu)}{dx} \to \frac{du(k_j, \widehat{m})}{dx}, \ \text{ in } L^2(0,1), \tag{40}$$

as $\nu \to \infty$, for all $i, j = 1, \ldots, N$. Finally, for all $i, j = 1, \ldots, N$ we obtain that

$$\lim_\nu \phi_{ij}(m_\nu) = \lim_\nu \left| \int u_i(m_\nu)' \overline{u_j(m_\nu)'} dx - S_{ij}^{obs.} \right|^2 =$$

$$\left| \int u_i(\widehat{m})' \overline{u_j(\widehat{m})'} dx - S_{ij}^{obs.} \right|^2 = \phi_{ij}(\widehat{m}),$$

since the absolute value function is continuous and the following limit exists,

$$\lim_{\nu} \int_0^1 u_i(m_\nu)' \overline{u_j(m_\nu)'} dx \in \mathbb{C}. \tag{41}$$

Therefore by the strong convergence of the sequences $(\phi_{ij}(m_\nu)_\nu,\ i, j = 1, \ldots, N$ and the weak lower semicontinuity of the norm, we obtain

$$\mu = \lim_{\nu} \phi(m_\nu) \geq \liminf_{\nu} \phi(m_\nu) = \sum_{ij=1}^{N} \phi_{ij}(\widehat{m}) + \frac{\varepsilon}{2} \liminf_{\nu} \|m_\nu\|_{H^1}^2 \geq \phi(\widehat{m}) \geq \mu \tag{42}$$

□

3.2.2 Derivative of Misfit and Optimality Condition

Here we derive the first order optimality condition of the problem in the continuous setting. We first define the form

$$b(u, v) = \int_0^1 u' v' dx,\ u, v \in H^1(0, 1). \tag{43}$$

We obtain the following result.

Proposition 6 *Let $(i, j) \in \{1, \ldots, N\}^2$. Then the function $\phi_{ij} : H^1((0, 1); (0, \infty)) \to [0, \infty]$ as defined in relation (31) is C^1, with derivative at an m_0*

$$\langle D_m \phi_{ij}(m_0), h \rangle = Re(\{b(u_i(m_0), \overline{u_j(m_0)}) - S_{ij}^{obs}\}\{\langle b(\cdot, \overline{u_j(m_0)}), Du_i(m_0)h \rangle + \langle b(u_i(m_0), \cdot), D_m \overline{u_j(m_0)} h) \rangle\}),$$

for a direction $h \in H^1((0, 1); \mathbb{R})$.

Proof We know that if

$$q : H^1((0, 1); \mathbb{R}) \to \mathbb{C} \tag{44}$$

is differentiable, then

$$\frac{1}{2} \langle D_m |q(m_0)|^2, h \rangle = Re(q(m_0) \langle D_m q(m_0), h \rangle) \tag{45}$$

In our case, $q(m_0) = b(u_i(m_0), \overline{u_j(m_0)}) - S_{ij}$, with

$$\langle Db(u, v), (h, z) \rangle = b(u, z) + b(h, v) \tag{46}$$

at $(u, v) \in \{H^1(0, 1)\}^2$, at direction (h, z). Therefore

$$\langle D_m q(m_0), h \rangle =$$

$$\langle Db(u_i(m_0), \overline{u_j}(m_0)) \circ D_m(u_i(m_0), \overline{u_j}(m_0)), h \rangle =$$

$$\langle Db(u_i(m_0), \overline{u_j}(m_0)), D_m(u_i(m_0), \overline{u_j}(m_0))h\rangle =$$

$$b(\overline{D_m u_j(m_0)h}, u_i(m_0)) + b(D_m u_i(m_0)h, \overline{u_j}(m_0)) =$$

$$\langle b(u_i(m_0), \cdot), \overline{D_m u_j(m_0)h})\})\rangle + \langle b(\cdot, \overline{u_j(m_0)}), Du_i(m_0)h\rangle. \tag{47}$$

□

We define $\mathcal{G} : H^1(0,1) \to H^1(0,1)'$ such that

$$\langle \mathcal{G}\phi, u\rangle = \int_0^1 u'\overline{\phi'}dx = b(u, \overline{\phi}). \tag{48}$$

This gives for a direction $h \in H^1((0,1);\mathbb{R})$

$$b(\overline{D_m u_j(m_0)h}, u_i(m_0)) = \overline{b(D_m u_j(m_0)h, \overline{u_i(m_0)})} =$$

$$\overline{\langle \mathcal{G}u_i, D_m u_j h\rangle} = \overline{\langle (D_m u_j)^* \mathcal{G}u_i, h\rangle}.$$

Since $h = \overline{h}$ (h is real), we obtain the following (see [22, page 37])

$$\langle \overline{(D_m u_j)^* \mathcal{G}u_i}, h\rangle = \overline{\langle (D_m u_j)^* \mathcal{G}u_i, \overline{h}\rangle} =$$

$$\overline{\langle (D_m u_j)^* \mathcal{G}u_i, h\rangle}. \tag{49}$$

We obtain similarly,

$$b(D_m u_i(m_0)h, \overline{u_j}(m_0)) = \langle (D_m u_i)^* \mathcal{G}u_j, h\rangle$$

Combining the above results we obtain the following theorem.

Theorem 7 *The function $\phi : H^1((0,1);(0,\infty)) \to [0,\infty]$, as defined in (29), is C^1, with derivative at an m_0*

$$D_m\phi(m_0) = \sum_{i,j=1}^{N} Re\Big(\Big\{\overline{(D_m u_j)^* \mathcal{G}u_i} + (D_m u_i)^* \mathcal{G}u_j\Big\}(b(u_i(m_0), \overline{u_j(m_0)}) - S_{ij}^{obs.})\Big) +$$

$$\varepsilon(m_0, \cdot)_{H^1(0,1)}.$$

Remark 5 Since we have derived the analytical expression of the F-derivative of ϕ, then the optimality condition is a variational inequality of the form,

$$\langle D_m\phi(\widehat{m}), m - \widehat{m}\rangle \geq 0, \ \forall m \in \mathbb{K}_{ad}, \tag{50}$$

with $D_m\phi(\widehat{m})$ given above at a local minimizer, $\widehat{m}$.

4 Numerical Results

In this section we include a number of numerical experiments/comparisons between the ROM based FWI method and the conventional FWI method. Before doing so, we include a paragraph regarding the discrete optimality condition of the ROM based misfit functional. In the numerical implementation below we use finite elements of "hat-funtion" type to approximate the solution of the differential equation.

4.1 Numerical Implementation: Discrete Optimality Condition

In this paragraph we derive the discrete optimality condition that we use for the numerical computation of the gradient of the ROM based misfit. In the discrete case, given L, a first order finite-difference matrix and $\eta = 1/N_x$ being the length of the spatial discretisation (N_x spatial points) we have that

$$S_{ij} = \eta(Lu_i, Lu_j)_{\mathbb{C}^{N_x}}, \tag{51}$$

assuming that we realize $(u_i)_{i=1}^N$ discretely. Now, in order to follow similar steps as in the continuous case, we take a direction $h \in \mathbb{R}^n$ and we consider as before, $\phi = \sum_{i,j=1}^N \phi_{ij}$ (for simplicity we do not use any regularization, thus we take $\varepsilon = 0$).

$$(D_m\phi_{ij}(m_0), h)_{\mathbb{R}^n} = Re\{(D_m(S_{ij}(m_0) - S_{ij}^{obs.}), D_m S_{ij}(m)h)_{\mathbb{C}^{N_x}}\} =$$

$$Re\{((D_m S_{ij}(m))^*\{S_{ij}(m_0) - S_{ij}^{obs.}\}, h)_{\mathbb{C}^{N_x}})\}. \tag{52}$$

We obtain that

$$D_m S_{ij} = \eta(D_m u_j)^* L^* L u_i + \eta u_j^* L^* L(D_m u_i) \Rightarrow \tag{53}$$

$$(D_m S_{ij})^* = \eta u_i^* L^* L(D_m u_j) + \eta(D_m u_i)^* L^* L u_j. \tag{54}$$

Also,

$$D_m\phi_{ij} = Re\{\eta(u_i^* L^* L(D_m u_j) + \eta(D_m u_i)^* L^* L u_j)[S_{ij} - S_{ij}^{obs.}]\}. \tag{55}$$

Now,

$$\eta u_i^* L^* L(D_m u_j) = \eta(L(D_m u_j), Lu_i)_{\mathbb{C}^{N_x}} = \eta\overline{(Lu_i, LD_m u_j)_{\mathbb{C}^{N_x}}} = \eta\overline{D_m u_j^* L^* L u_i}, \tag{56}$$

therefore we get

$$D_m\phi_{ij} = \eta Re\{[S_{ij} - S_{ij}^{obs.}](\overline{D_m u_j^* L^* L u_i} + (D_m u_i)^* L^* L u_j)\}$$

Remark 6 In stead of using a variational inequality as our optimality conditions, we can seek for simplicity solutions such that $D_m\phi(\widehat{m}) = 0$.

Remark 7 In the continuous case we defined an operator $\mathcal{G}$ such that

$$\langle \mathcal{G}\phi, u\rangle = \int_0^1 \overline{\partial_x\phi}\partial_x u dx. \tag{57}$$

In the discrete sense this means that

$$\langle \mathcal{G}\phi, u\rangle \approx \eta(L\overline{\phi}, Lu)_{\mathbb{R}^{N_x}} = \eta(L^* L\overline{\phi}, u)_{\mathbb{R}^{N_x}} = \eta\phi^* L^* L u,$$

where L^* is the adjoint of L defined by the inner product, $(\bar{\cdot}, \cdot)$.

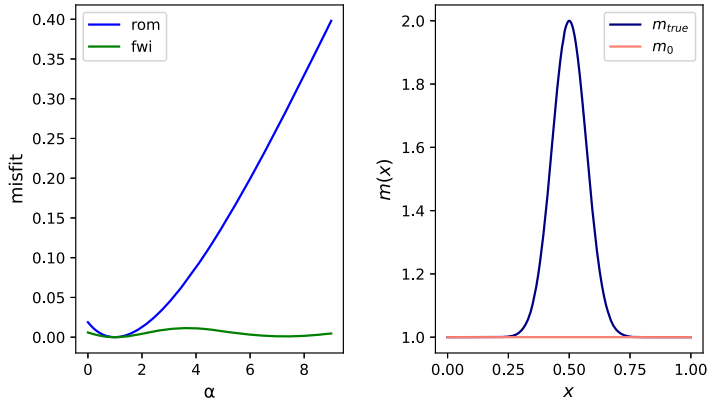

Fig. 1 Comparison between the ROM based FWI and the conventional FWI when we use 10 wavenumbers with $k_{min} = 18$ and $k_{max} = 24$. On the right we show m_0 and m_{true}

4.2 Comparison with Conventional FWI: Convexity

In this section we compare our ROM based FWI approach with the conventional FWI. We use double sided data for both methods. We can now consider u as a function of discrete values of x (assuming as before N_x amount of spatial nodes). We also recall that we use N-samples of the wavenumber. We formulate the FWI problem as follows; given band-limited observations $z_i \in \mathbb{C}^2,\ i = 1, \ldots, N$, with

$$z_i = (f(k_i), g(k_i)),\ i = 1, \ldots, N,$$

and sampling matrix

$$P = \begin{pmatrix} 1 & 0 & \cdots 0 \\ 0 & 0 & \cdots 1 \end{pmatrix} \in \mathbb{R}^{2 \times N_x},$$

find m such that the following functional

$$\phi_{fwi}(m) = \frac{1}{2} \sum_{i=1}^{N} \| Pu(k_i, m) - z_i \|_2^2$$

is minimized. As we shall see in the chosen examples, the ROM based method has a convex profile that avoids local minimizers of the conventional FWI functional. We showcase that by performing three experiments. In the first two we use measurements corresponding to relatively high wavenumbers compared to the maximum value of the respective m. In the last one we use both high wavenumber measurements and strong contrast.

We show that the ROM based FWI misfit avoids the local minimizers of the FWI functional by plotting the values of the two misfits as functions of m, when $m = m_0 + adm$, with $m_0 = 1$, and with a having range in an interval I_a such that there exists $a' \in I_a$ with $m_{\text{true}} = m_0 + a'dm$, $(dm = m_{\text{true}} - m_0)$. We observe that in the first two examples the ROM misfit functional is convex (figures 1, 2). In the third example the functional is not convex, but the local minimizers of the conventional FWI are avoided (figure 3). Possibly, the rank-2 terms that are included in the stiffness matrix convexify the misfit functional by

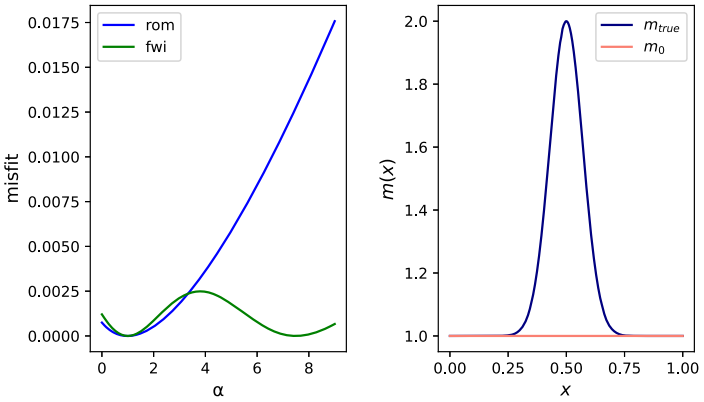

Fig. 2 Comparison between the ROM based FWI and the conventional FWI when we use 2 wavenumbers $k = 20, 20.1$. On the right we show m_0 and m_{true}

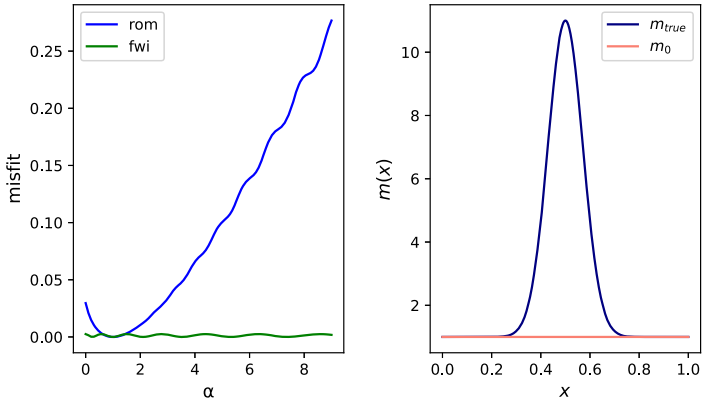

Fig. 3 Comparison between the ROM based FWI and the conventional FWI when we use 2 wavenumbers with $k = 20, 20.1$. On the right we show m_0 and m_{true}

reducing the nonlinearity. It is important to notice that in similar works, see for example [14], the observed reduction of the nonlinearity of the misfit functional could be, at least partly, due to the transformation of the ROM system using the Lanczos algorithm. Keep in mind though that in our case, without the use of impedance type boundary conditions, the stiffness matrix depends linearly on the data, thus we do not expect any improvements on the convexity compared to the traditional FWI method.

4.3 Comparison with Conventional FWI: Reconstruction of a Smooth Coefficient

We split this section in two parts. In the first part we compare the two methods assuming that we have access to noiseless measurements. In the second part we add noise to the measurements.

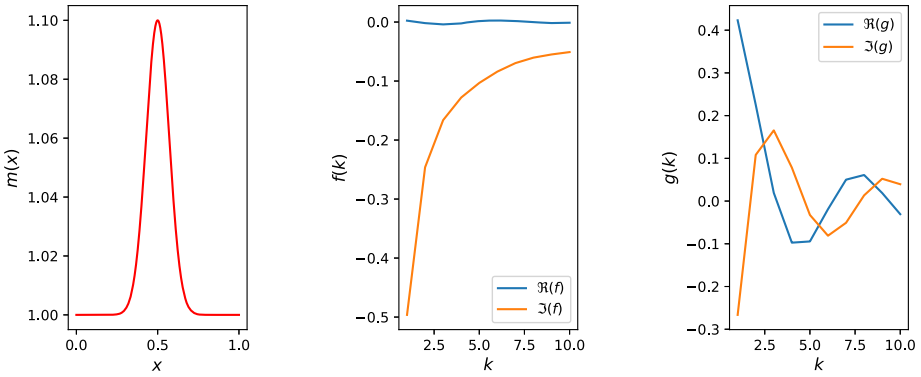

Fig. 4 From left to right. The coefficient, the reflection data f, the transmission data g

4.3.1 Reconstruction Using Noiseless Data

Following the standard adjoint state method, we present the numerical reconstruction of a refractive index using the ROM based FWI. For the numerical reconstruction we use a standard fixed point iteration of the form

$$m^{(\kappa+1)} = m^{(\kappa)} - \omega D_m \phi(m^{(\kappa)}),\ \kappa = 1, 2, \ldots, \tag{58}$$

with step ω. In Fig. 4 we show the refractive index of our experiment, the reflection and the transmission data. We compare the results of our method with the results of the conventional FWI method using the same step ω for both metods, and when we run the fixed point iteration for 15, 30 and 45 steps. Results can be seen in Figs. 5-7. Finally, Fig. 8 shows that after a sufficiently large number of iterations, the ROM based method recovers a coefficient that is closer to the true one. Also, the data fit of the reflection data is slightly better when we follow the ROM based method. The data fit of the transmission data does not seem to improve when following the ROM based method.

4.3.2 Reconstrunction with Noise in the Data

In this subsection we compare the methods on noisy data. We add i.d.d. normally distributed noise to the data with mean zero and variance σ^2. We study the case when $\sigma = 1 \times 10^{-4}$. We do not add any additional regularization. The results are shown in Fig. 9. We observe that the ROM based approach is affected by the noise and it yields inferior results compared with the conventional FWI method.

5 Conclusion and Discussion

In this paper we studied a nonlinear optimization problem which can be viewed as a modified FWI problem using the stiffness ROM matrix as input. Due to the unconventional form of the misfit functional that includes not weakly lower semicontinuous terms, we studied well-posedness of the problem and we compared numerically our proposed method with the conventional FWI method. As we observed through our numerical experiments, the ROM based FWI misfit functional seems to have a convex profile, something that the conventional

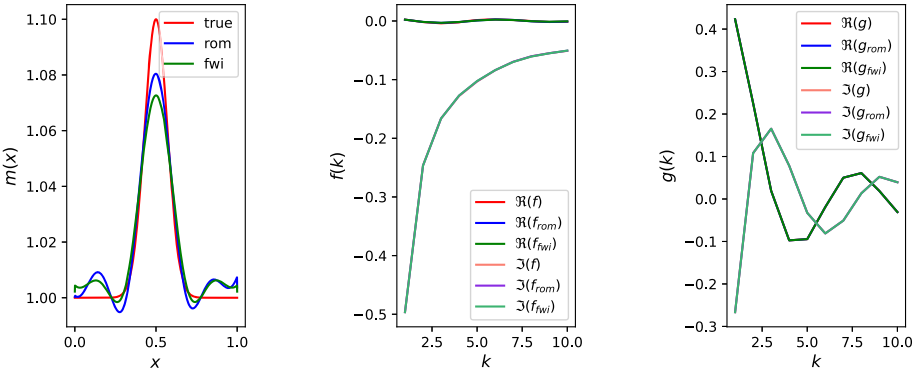

Fig. 5 Comparison between the results produced by the ROM based and conventional FWI methods after 15 steps of the fixed point iteration. On the left, comparison between reconstructed coefficients. The errors are $\|m_{rom} - m\|_2 = 0.214$ and $\|m_{fwi} - m\|_2 = 0.271$. In the middle and on the right we compare data-fit (transmission and reflection)

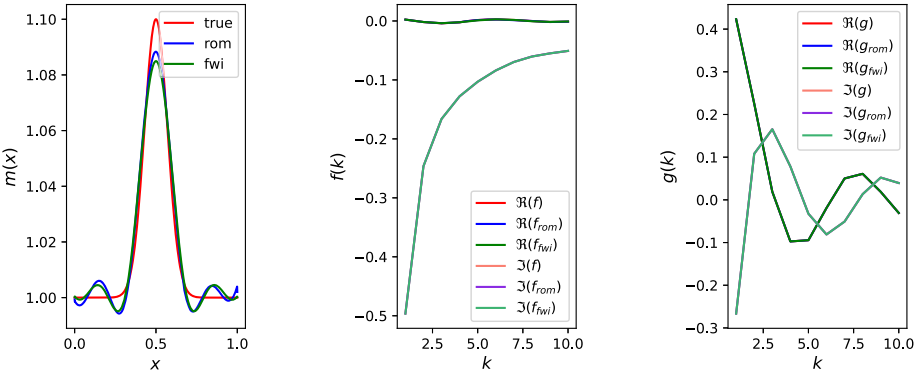

Fig. 6 Comparison between the results produced by the ROM based and con- ventional FWI methods after 30 steps of the fixed point iteration. On the left, comparison between reconstructed coefficients. The errors are $\|m_{rom} - m\|_2 = 0.152$ and $\|m_{fwi} - m\|_2 = 0.169$. In the middle and on the right we compare data-fit (transmission and reflection)

FWI lacks when we use relatively high frequency data. This observed convex behaviour of the ROM based functional makes the extension of the method to 2 and 3 dimensional inverse problems for the Helmholtz equation interesting. With this paper we believe that we have made the first steps towards this extension. Of course, different variations of the ROM based FWI methods can be proposed, in the sense of using M (or even B) as input. However, despite the possible limitations of using the Lanczos method within the framework of this paper, it would be interesting to investigate potential combinations of the Lanczos method with the ROM based FWI approach. For example it would be interesting to study a method that compares the misfit between the Lanczos orthogonalized ROM and its counterpart that corresponds to the modeled parameter. In any case, one should be aware of the possible issues regarding the stability of the Lanczos algorithm. The study of these cases are interesting and in the future we plan on analysing these variations. Finally, it is worth noting that our method might have some desired properties, such as improved convexity of the misfit for

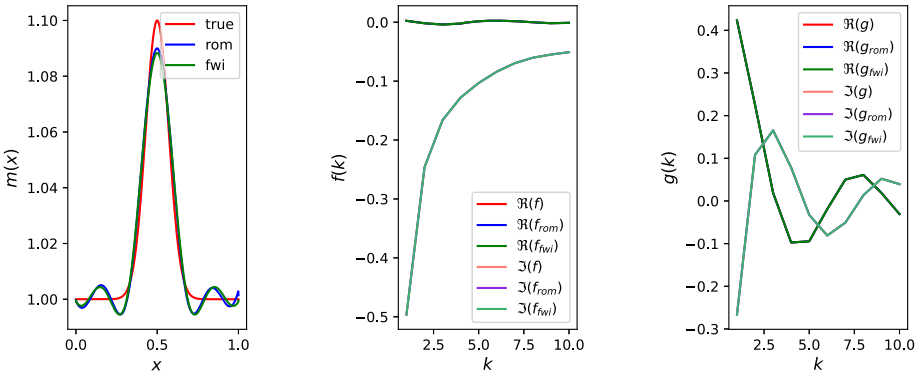

Fig. 7 Comparison between the results produced by the ROM based and con- ventional FWI methods after 45 steps of the fixed point iteration. On the left, comparison between reconstructed coefficients. The errors are $\|m_{rom} - m\|_2 = 0.145$ and $\|m_{fwi} - m\|_2 = 0.156$. In the middle and on the right we compare data-fit (transmission and reflection)

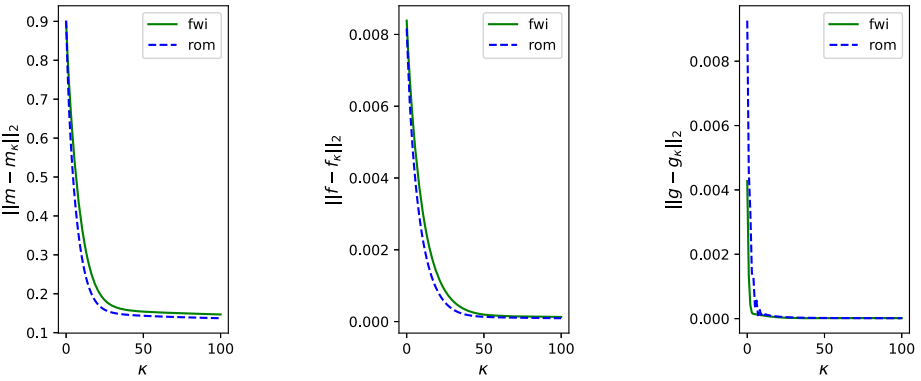

Fig. 8 From left to right. On the left, comparison of the misfit $\|m - m_\kappa\|_2$ when m_κ is recovered doing $\kappa-$ steps of the fixed point iterations either of the conventional or the ROM based FWI method. We compare similarly the misfits of the reflection and the transmission data yielded by the respective m_κ. We used the same step ω in both fixed point iterations

example, but it is sensitive in the presence of noise. We also plan to investigate various ways of improving the performance of the ROM based FWI method when the measurements are not exact.

Appendix: Proofs

A.1 Proof of Proposition 1

Proof of Proposition 1 For the sake of completeness we include a sketch of the proof. We refer to [17] and [18] for more details. We define the forms $a_1, a_2 : H^1(0,1)^2 \to \mathbb{C}$ with

$$a_1(u,v) = \int_0^1 u'\overline{v'}dx - ik\{(u\overline{v})|_{x=0} + (u\overline{v})|_{x=1}\}, \tag{A1}$$

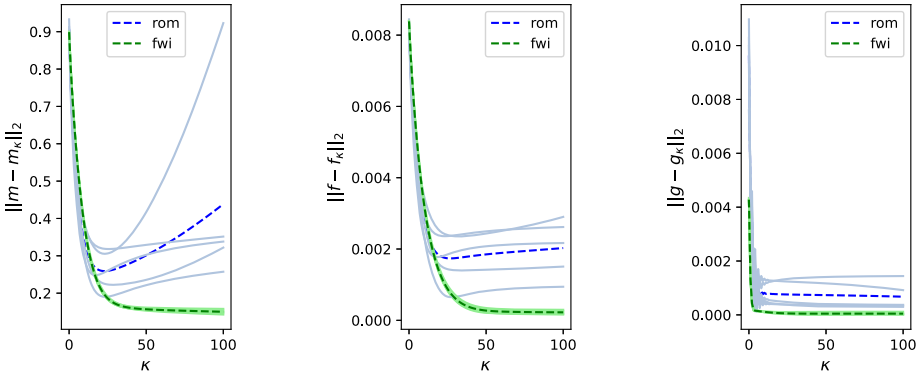

Fig. 9 Comparison of the two methods when there is noise in the measurements ($\sigma = 1 \times 10^{-4}$). On the left, comparison of the misfit $\|m - m_\kappa\|_2$ when m_κ is recovered doing $\kappa-$ steps of the fixed point iterations either of the conventional or the ROM based FWI method (dotted lines show average of 5 experiments). We compare similarly the average of the misfits of the reflection and the transmission data yielded by the respective m_κ. We used the same step in both fixed point iterations

$$a_2(u, v) = -\int_0^1 mu\overline{v}dx,\ u, v \in H^1(0, 1). \tag{A2}$$

We note that a_1 is coercive and that a_1, a_2 are bounded forms. For a_1, we denote with L, U the low bound in the coercivity estimate, and the upper bound for the continuity estimate respectively. We define the linear Riesz isomorphism,

$$\Phi : H^1(0, 1) \to \overline{H^1(0, 1)}', \tag{A3}$$

with $\Phi u = (u, \cdot)_{H^1}, u \in H^1(0, 1)$. Since $a_1(u, \cdot)$ is an antilinear functional on $H^1(0, 1)$, and using the Riesz representation theorem we define $\mathcal{T} : H^1(0, 1) \to H^1(0, 1)$ with

$$a_1(u, v) = (\mathcal{T}u, v)_{H^1}. \tag{A4}$$

$\mathcal{T}$ is one-to-one onto and we have the estimates $\|\mathcal{T}\|_\infty \leq U,\ \|\mathcal{T}^{-1}\|_\infty \leq L$. Also, we define the linear operator $\mathcal{V} : L^2(0, 1) \to \overline{H^1(0, 1)}',\ s \overset{\mathcal{V}}{\mapsto} a_2(u, \cdot)$. We also define the linear map

$$\mathcal{A}_1 = \mathcal{T}^{-1}\Phi^{-1}\mathcal{V} : L^2(0, 1) \to H^1(0, 1) \tag{A5}$$

and

$$\mathcal{A} = \mathcal{A}_1 \circ i_{H^1 \to L^2} : H^1(0, 1) \overset{c}{\hookrightarrow} L^2(0, 1) \to H^1(0, 1),\ s \mapsto \mathcal{A}_1 s. \tag{A6}$$

$\mathcal{A}$ is bounded as composition of bounded operators. Also, for $s \in H^1(0, 1), w \in H^1(0, 1)$, we have $a_1(\mathcal{A}s, w) = a_2(s, w)$. We claim that $\mathcal{I} + k^2\mathcal{A}$ is one-to-one. Let now $u \in H^1(0, 1)$. Finding a solution of the differential equation, is equivalent to finding $u \in H^1(0, 1)$ that satisfies

$$a_1(u, v) + k^2 a_2(u, v) = -\langle \delta_0, v\rangle, \forall v \in H^1(0, 1) \iff$$
$$a_1(u, v) + k^2 a_1(\mathcal{A}u, v) = -\langle \delta_0, v\rangle,\ \forall v \in H^1 \iff$$

$$a_1(u+k^2\mathcal{A}u,v)=-\langle\delta_0,v\rangle,\ \forall v\in H^1 \iff \tag{A7}$$

$$(\mathcal{T}(u+k^2\mathcal{A}u),v)_{H^1(0,1)}=-\langle\delta_0,v\rangle,\ \forall v\in H^1 \Rightarrow \tag{A8}$$

$$\Phi\mathcal{T}(\mathcal{I}+k^2\mathcal{A})u\overset{\overline{H^1(0,1)}'}{=}-\delta_0 \iff (\mathcal{I}+k^2\mathcal{A})u=\mathcal{T}^{-1}\Phi^{-1}(-\delta_0)\in H^1(0,1). \tag{A9}$$

Since $\mathcal{A}\in\mathcal{L}(H^1(\Omega),H^1(\Omega))$ is compact and $\mathcal{I}+k^2\mathcal{A}$ is injective, using the Fredholm alternative we obtain that there exists a unique element $u\in H^1(\Omega)$ that satisfies the last equation. Finally, we obtain the forward stability estimate

$$\|u\|_{H^1(0,1)}\leq\|(\mathcal{I}+k^2\mathcal{A})^{-1}\|_{\mathcal{L}(H^1,H^1)}\|\mathcal{T}^{-1}\|_{\mathcal{L}(H^1,H^1)}\|\Phi^{-1}\|_{\mathcal{L}(H^1,\overline{H^1}')}\|\delta_0\|_{\overline{H^1}'}.$$

□

Remark 8 Observe that we even if we assume that $m>0$ is bounded, then we can still show existence and uniqueness of solutions of the forward problem.

A.2 Proof of Lemma 3

Proof of Lemma 3 We take $k=k_i$ and we write $u_i=u(k_i,\cdot)$. Take $\phi=u_j$,

$$(u_i',u_j')-k_i^2(mu_i,u_j)-\imath k_iu_i(1)\overline{u_j(1)}-\imath k_iu_i(0)\overline{u_j(0)}=-\overline{u_j(0)} \tag{A10}$$

Now we denote

$$M_{ij}=(mu_i,u_j) \tag{A11}$$

$$S_{ij}=(u_i',u_j') \tag{A12}$$

and we obtain

$$S_{ij}-k_i^2M_{ij}=-\overline{f_j}+\imath k_i\{g_i\overline{g_j}+f_i\overline{f_j}\} \tag{A13}$$

Similarly for $k=k_j$

$$(u_j',u_i')-k_j^2(mu_j,u_i)-\imath k_ju_j(1)\overline{u_i(1)}-\imath k_ju_j(0)\overline{u_i(0)}=-\overline{u_i(0)}, \tag{A14}$$

which gives

$$S_{ji}-k_j^2M_{ji}=-\overline{f_i}+\imath k_j\{g_j\overline{g_i}+f_j\overline{f_i}\}. \tag{A15}$$

Taking the complex conjugate of the above relation we obtain

$$\overline{S_{ji}-k_j^2M_{ji}}=$$

$$S_{ij}-k_j^2M_{ij}=-f_i-\imath k_j\{g_i\overline{g}_j+f_i\overline{f}_j\}. \tag{A16}$$

Subtracting (A13) - (A16) we arrive at

$$S_{ij}-k_i^2M_{ij}-S_{ij}+k_j^2M_{ij}=$$

$$-\overline{f_j}+\imath k_i\{g_i\overline{g_j}+f_i\overline{f_j}\}+f_i+\imath k_j\{g_i\overline{g}_j+f_i\overline{f}_j\}\}\Rightarrow$$

$$(-k_i^2+k_j^2)M_{ij}=-\overline{f_j}+f_i+\imath k_i\{g_i\overline{g_j}+f_i\overline{f_j}+f_i\}+\imath k_j\{g_i\overline{g_j}+f_i\overline{f_j}\}\Rightarrow \tag{A17}$$

$$M_{ij}=\frac{-\overline{f_j}+f_i+\imath k_i\{g_i\overline{g_j}+f_i\overline{f_j}\}+\imath k_j\{g_i\overline{g_j}+f_i\overline{f_j}\}}{k_j^2-k_i^2}\Rightarrow \tag{A18}$$

$$M_{ij}=-\frac{\overline{f_j}-f_i}{k_j^2-k_i^2}+\imath\frac{(k_i+k_j)(g_i\overline{g_j}+f_i\overline{f}_j)}{k_j^2-k_i^2}\Rightarrow \tag{A19}$$

$$M_{ij}=-\frac{\overline{f_j}-f_i}{k_j^2-k_i^2}+\imath\frac{g_i\overline{g_j}+f_i\overline{f_j}}{k_j-k_i}. \tag{A20}$$

Similarly we multiply (A13) by k_j^2 and (A16) by k_i^2 and we obtain

$$k_j^2S_{ij}-k_j^2k_i^2M_{ij}=-k_j^2\overline{f_j}+\imath k_j^2k_i\{g_i\overline{g_j}+f_i\overline{f_j}\} \tag{A21}$$

$$k_i^2S_{ij}-k_j^2k_i^2M_{ij}=-k_i^2f_i-\imath k_i^2k_j\{g_i\overline{g}_j+f_i\overline{f}_j\} \tag{A22}$$

Subtracting the above two relations,

$$(k_j^2-k_i^2)S_{ij}=-k_j^2\overline{f_j}+\imath k_j^2k_i\{g_i\overline{g_j}+f_i\overline{f_j}\}+k_i^2f_i+\imath k_i^2k_j\{g_i\overline{g}_j+f_i\overline{f}_j\}\Rightarrow \tag{A23}$$

$$S_{ij}=\frac{-k_j^2\overline{f_j}+k_i^2f_i}{k_j^2-k_i^2}+\imath(k_j^2k_i+k_i^2k_j)\frac{g_i\overline{g}_j+f_i\overline{f}_j}{k_j^2-k_i^2}\Rightarrow \tag{A24}$$

$$S_{ij}=-\frac{k_j^2\overline{f_j}-k_i^2f_i}{k_j^2-k_i^2}+\imath(k_j^2k_i+k_i^2k_j)\frac{g_i\overline{g}_j+f_i\overline{f}_j}{k_j^2-k_i^2} \tag{A25}$$

Now, for the diagonal elements of M. First of all, consider

$$\int_0^1 mu(\lambda)\overline{u(\mu)}dx:=\mathcal{M}(\lambda,\mu):[\lambda_{\min},\lambda_{\max}]\times[\mu_{\min},\mu_{\max}]\to\mathbb{C}. \tag{A26}$$

$\mathcal{M}$ is a continuous function, thus, if we fix $\mu=\mu_0$, then the following limit exists

$$\lim_{\lambda\to\mu_0}M(\lambda,\mu_0)=\|u(\mu_0)\|_{L^2(0,1,mdx)}>0 \tag{A27}$$

The elements of the mass matrix $\mathcal{M}$ are given by relation (A20) above. Let $k_i^2=\lambda$ and $k_j^2=\lambda+h$, with $h\in\mathbb{R}$. Take

$$M_{ij}=M(\lambda,\lambda+h)=-\frac{\overline{f(\lambda+h)}-f(\lambda)}{h}+\imath\frac{g(\lambda)\overline{g(\lambda+h)}+f(\lambda)\overline{f(\lambda+h)}}{\sqrt{\lambda+h}-\sqrt{\lambda}} \tag{A28}$$

We write $f=Re(f)+\imath Im(f)$ and $g=Re(g)+\imath Im(g)$. The first term of (A28) expression can be written as

$$-\frac{\overline{f(\lambda+h)}-f(\lambda)}{h}=-\frac{Re(f)(\lambda+h)-\imath Im(f)(\lambda+h)-Re(f)(\lambda)-\imath Im(f)(\lambda)}{h}=$$

$$-\frac{Re(f)(\lambda+h)-Re(f)(\lambda)}{h}+\imath\frac{Im(f)(\lambda+h)+Im(f)(\lambda)}{h}. \tag{A29}$$

The second term of (A28) is

$$\iota \frac{g(\lambda)\overline{g(\lambda+h)}+f(\lambda)\overline{f(\lambda+h)}}{\sqrt{\lambda+h}-\sqrt{\lambda}} =$$

$$\iota \frac{Re(g)Re(g^h)+Im(g)Im(g^h)+Re(f)Re(f^h)+Im(f)Im(f^h)}{\sqrt{\lambda+h}-\sqrt{\lambda}}+$$

$$\Big(-\frac{Im(g)Re(g^h)-Re(g)Im(g^h)+Im(f)Re(f^h)-Re(f)Im(f^h)}{\sqrt{\lambda+h}-\sqrt{\lambda}}\Big), \tag{A30}$$

since

$$g\bar{g_h} = (Re(g)+\iota Im(g))(Re(g^h)-\iota Im(g^h)) =$$

$$Re(g)Re(g)^h + Im(g)Im(g)^h + \iota Im(g)Re(g^h) - \iota Im(g^h)Re(g),$$

where we used the shorthand notation $f^h = f(\lambda+h)$ (also for g). Now, since this limit exists,

$$\lim_{h\to 0} M(\lambda,\lambda+h) = \|u(\lambda)\|_{L^2(0,1,mdx)} \in \mathbb{R},$$

we obtain that

$$\lim_{h\to 0} \Im(M(\lambda,\lambda+h)) = 0, \tag{A31}$$

thus

$$\lim_{h\to 0}\Big\{\frac{Im(f)^h+Im(f)}{h}+$$

$$\frac{Re(g)Re(g)^h+Im(g)Im(g)^h+Re(f)Re(f)^h+Im(f)Im(f)^h}{\sqrt{\lambda+h}-\sqrt{\lambda}}\Big\}=0.$$

Therefore

$$M_{ii} = \lim_{h\to 0}\Big\{-\frac{Re(f)(\lambda+h)-Re(f)(\lambda)}{h}-$$

$$\frac{Im(g)Re(g)^h-Re(g)Im(g)^h+Im(f)Re(f)^h-Re(f)Im(f)^h}{\sqrt{\lambda+h}-\sqrt{\lambda}}\Big\}=$$

$$\lim_{h\to 0}\Big\{-\frac{Re(f)(\lambda+h)-Re(f)(\lambda)}{h}-$$

$$\frac{Im(g)Re(g)^h-Re(g)Im(g)+Re(g)Im(g)-Re(g)Im(g)^h}{\sqrt{\lambda+h}-\sqrt{\lambda}}-$$

$$\frac{Re(f)Im(f)^h-Im(f)Re(f)^h}{\sqrt{\lambda+h}-\sqrt{\lambda}}\Big\}\Rightarrow$$

$$M_{ii} = -\frac{dRe(f)}{d\lambda}(\lambda) - Im(g)(\lambda)2\sqrt{\lambda}\frac{dRe(g)}{d\lambda}(\lambda) + Re(g)(\lambda)2\sqrt{\lambda}\frac{dIm(g)(\lambda)}{d\lambda}-$$

$$Im(f)(\lambda)2\sqrt{\lambda}\frac{dRe(f)}{d\lambda}(\lambda) + Re(f)(\lambda)2\sqrt{\lambda}\frac{dIm(f)(\lambda)}{d\lambda}. \tag{A32}$$

This relation can be simplified even more as

$$M_{ii} = -\frac{dRe(f)}{d\lambda}(\lambda) + 2\sqrt{\lambda}Im\left\{\overline{g(\lambda)}\frac{dg}{d\lambda}(\lambda) + \overline{f(\lambda)}\frac{df}{d\lambda}(\lambda)\right\}. \tag{A33}$$

We compute the diagonal of S similarly. □

A.3 Proof of Lemma 4

We start by stating the implicit function theorem.

Theorem 8 *Let a function $\tilde{F} : C \times P \to W$, C, P, W being Banach spaces. We assume that there exists an open set $C_0 \subset C$ such that for every $m \in C_0$ there exists a unique $u = u(m) \in P$ such that*

$$\tilde{F}(m, u) = 0. \tag{A34}$$

Then if

$$\tilde{F} : C \times P \to W \tag{A35}$$

is continuous, if

$$\partial_2\tilde{F} : C \times P \to W \tag{A36}$$

is continuous and if

$$(\partial_2\tilde{F}(m, u))^{-1} : W \to P, \ \forall m \in C_0, \tag{A37}$$

exists and is bounded, then there exists a continuous map such that

$$C_0 \ni m \mapsto u(m) \in P. \tag{A38}$$

Also, if $\partial_1\tilde{F}$ is continuous, we obtain that u is Fréchet differentiable.

Lemma 9 *The requirements of theorem A.3 hold for F.*

Proof Let $P = H^1(0, 1)$. For all $m \in C_0 = C([0, 1]; (0, \infty)) \subset C = C([0, 1]; \mathbb{R})$ there exists u such that $F(m, u) = 0$. Second, we want to show continuity of F. We get for $(\delta m, \delta u) \in C \times H^1$

$$F(m + \delta m, u + \delta u) - F(m, u) =$$

$$\mathcal{S}(u + \delta u) - k^2\mathcal{M}(m + \delta m)(u + \delta u) - \imath k\mathcal{B}(u + \delta u) + \delta_0 -$$

$$(\mathcal{S}(u) - k^2\mathcal{M}(m)(u) - \imath k\mathcal{B}(u) + \delta_0) =$$

$$\mathcal{S}(\delta u) - k^2\mathcal{M}(\delta m)(u) - k^2\mathcal{M}(m)(\delta u) - k^2\mathcal{M}(\delta m)(\delta u) - \imath k\mathcal{B}(\delta u). \tag{A39}$$

Now, for $\phi \in H^1(0,1)$

$$|\langle \mathcal{M}(\delta m)(u), \phi\rangle| = \left| \int_0^1 (\delta m) u \overline{\phi} dx \right| \leq \|\delta m\|_\infty \int_0^1 \left| u\overline{\phi} \right| dx \leq$$

$$\|\delta m\|_\infty \|u\|_\infty \int_0^1 \left| \overline{\phi} \right| dx \leq \|\delta m\|_\infty \|u\|_\infty \|\phi\|_\infty \leq \gamma^2 \|\delta m\|_\infty \|u\|_{H^1} \|\phi\|_{H^1},$$

where γ is the bound of the Sobolev imbedding from H^1 to $C[0,1]$. Similarly,

$$|\langle \mathcal{M}(m)(\delta u), \phi\rangle| \leq \gamma^2 \|\delta u\|_{H^1} \|m\|_\infty \|\phi\|_{H^1}, \tag{A40}$$

$$|\langle \mathcal{M}(\delta m)(\delta u), \phi\rangle| \leq \gamma^2 \|\delta u\|_{H^1} \|\delta m\|_\infty \|\phi\|_{H^1}. \tag{A41}$$

Also,

$$|\langle \mathcal{S}\delta u, \phi\rangle| = |(\delta u', \phi')| \leq \|\delta u'\|_{L^2} \|\phi'\|_{L^2} \leq \|\delta u\|_{H^1} \|\phi\|_{H^1}, \tag{A42}$$

$$|\langle \mathcal{B}(\delta u), \phi\rangle| = |(\delta u \phi)|_{x=0} + (\delta u \phi)|_{x=1}| \leq \|\delta u\|_\infty \|\phi\|_\infty + \|\delta u\|_\infty \|\phi\|_\infty \leq$$
$$2\gamma \|\delta u\|_{H^1} \|\phi\|_{H^1}.$$

All the above relations yield that

$$\|F(m+\delta m, u+\delta u) - F(m,u)\|_{\overline{H^1}'} \to 0 \text{ as } \delta m, \delta u \to 0. \tag{A43}$$

Also, since for fixed m, $F(m,\cdot)$ is affine on u, we get that

$$\partial_2 F(m,u) \in \mathcal{L}(H^1, \overline{H^1}'),\ u \in H^1, \tag{A44}$$

and at a point (m,u) at a direction s we get

$$\partial_2 F(m,u)s = \langle (\mathcal{S} - k^2 \mathcal{M}(m) - \imath k \mathcal{B})s, \cdot\rangle,\ s \in H^1. \tag{A45}$$

As before, $\partial_2 F$ is continuous as a function of (m,u). Similarly, for fixed u, we obtain at (m,u) in a direction h

$$\partial_1 F(m,u)h = -k^2 \langle \mathcal{M}(u)h, \cdot\rangle \Rightarrow \tag{A46}$$

$$\partial_1 F(m,u)h = -k^2 \langle \mathcal{M}(u)h, \cdot\rangle,\ \forall (m,u) \in C \times H^1(0,1), \tag{A47}$$

and $\partial_1 F$ is continuous on $C \times H^1$. Since the partial derivatives of F are continuous we conclude that the gradient of F exists and is continuous. Finally, since at any point of evaluation,

$$\partial_2 F(m,u) = \mathcal{S} - k^2 \mathcal{M}(m) - \imath k \mathcal{B} = \Phi \mathcal{T} (\mathcal{I} + k^2 \mathcal{A}) \tag{A48}$$

is invertible, we obtain that the following map

$$C([0,1]; (0,\infty)) \ni m \mapsto u(k,m) \in H^1(0,1) \tag{A49}$$

is well-defined, continuous and is F-differentiable. □

Proof of Lemma 4 The proof of the lemma is a corollary of the above result □

Remark 9 Notice that

$$H^1((0,1);(0,\infty)) \ni m \mapsto u(k,m) \in H^1(0,1) \tag{A50}$$

will also be differentiable. Showing this assertion follows analogously as the proof of lemma 9 and by utilizing the embedding of $H^1(0,1)$ into $C[0,1]$. Notice also that $H^1((0,1);(0,\infty))$ is open in $H^1((0,1);\mathbb{R})$.

Acknowledgements Authors would like to thank Sjoerd Verduyn Lunel, Carolin Kreisbeck and Ivan Vasconcelos for their suggestions and the fruitful discussions. We would also like to thank the reviewers for their insightful suggestions and comments that helped us improve our manuscript.

Author Contribution Both authors contributed equally to this work.

Funding This work was supported by the Utrecht Consortium for Subsurface Imaging (UCSI).

Declarations

Ethics approval and consent to participate No experiments and/or research involving human participants and/or animals was performed.

Consent for publication The authors declare that the work has not been published before and that the work is not under consideration elsewhere.

Competing Interests The authors declare no conflict of interest.

References

1. Fink, J.P., Rheinboldt, W.C.: On the error behavior of the reduced basis technique for nonlinear finite element approximations. Z. Angew. Math. Mech. **63**, 21–28 (1983)
2. Maday, Y., Patera, A.T., Turinici, G.: A priori convergence theory for reduced-basis approximations of single-parameter elliptic partial differential equations. J. Sci. Comput. **17**, 437–446 (2002)
3. Veroy, K., Prud'homme, C., Rovas, D.V., Patera, A.T.: A posteriori error bounds for reduced-basis approximation of parametrized noncoercive and nonlinear elliptic partial differential equations (2003)
4. Sen, S., Veroy, K., Huynh, D.B.P., Deparis, S., Nguyen, N.C., Patera, A.T.: "natural norm" a posteriori error estimators for reduced basis approximations. J. Comput. Phys. **217**, 37–62 (2006)
5. Druskin, V., Moskow, S., Zaslavsky, M.: Lippmann–Schwinger–Lanczos algorithm for inverse scattering problems. Inverse Probl. **37** (2021)
6. Borcea, L., Druskin, V., Mamonov, A.V., Moskow, S., Zaslavsky, M.: Reduced order models for spectral domain inversion: Embedding into the continuous problem and generation of internal data. (2019). arXiv:1909.06460
7. Natterer, F.: A discrete Gelfand-levitan theory. (1989). http://wwwmath1.uni-muenster.de/num/Preprints/1998/natterer
8. Tataris, A., Leeuwen, T.: A distributional Gelfand–levitan–Marchenko equation for the Helmholtz scattering problem on the line. J. Math. Phys. **63**(10), Article ID 103507 (2022). https://doi.org/10.1063/5.0096920
9. Tataris, A., Leeuwen, T.: A regularised total least squares approach for 1d inverse scattering. Mathematics **10**(2) (2022). https://doi.org/10.3390/math10020216
10. Ware, J.A., Aki, K.: Continuous and discrete inverse-scattering problems in a stratified elastic medium. I. Plane waves at normal incidence. J. Acoust. Soc. Am. **45**(4), 911–921 (1969)
11. Burridge, R.: The Gelfand-levitan, the Marchenko, and the Gopinath-sondhi integral equations of inverse scattering theory, regarded in the context of inverse impulse-response problems. Wave Motion **2**(4), 305–323 (1980)

12. Koelink, E.: Scattering Theory. Radboud University (2008)
13. Borcea, L., Garnier, J., Mamonov, A.V., Zimmerling, J.T.: Waveform inversion via reduced order modeling. (2022). arXiv:2202.01824
14. Mamonov, A.V., Borcea, L., Garnier, J., Zimmerling, J.: Velocity estimation via model order reduction (2022). arXiv:2208.01209. https://doi.org/10.48550/ARXIV.2208.01209
15. Borcea, L., Garnier, J., Mamonov, A.V., Zimmerling, J.T.: Reduced order model approach for imaging with waves. Inverse Probl. **38** (2021)
16. Leeuwen, T., Tataris, A.: A data-driven approach to solving a 1D inverse scattering problem. AIP Adv. **13**(6), Article ID 065310 (2023). https://doi.org/10.1063/5.0154182
17. Wald, A., Schuster, T. Tomographic terahertz imaging using sequential subspace optimization. In: Hofmann, B., Leitão, A., Zubelli, J.P. (eds.) New Trends in Parameter Identification for Mathematical Models, pp. 261–290. Springer, Cham (2018). https://doi.org/10.1007/978-3-319-70824-9_14
18. Bao, G., Li, P.: Inverse medium scattering for the Helmholtz equation at fixed frequency. Inverse Probl. **21**(5), 1621–1641 (2005). https://doi.org/10.1088/0266-5611/21/5/007
19. Druskin, V., Moskow, S., Zaslavsky, M.: On extension of the data driven rom inverse scattering framework to partially nonreciprocal arrays. Inverse Probl. (2022)
20. Hungerländer, P., Kaltenbacher, B., Rendl, F.: Regularization of inverse problems via box constrained minimization. Inverse Probl. Imaging **14**(3), 437–461 (2020)
21. Connolly, T.J., Wall, D.J.N.: On frechet differentiability of some nonlinear operators occurring in inverse problems: an implicit function theorem approach. Inverse Probl. **6**(6), Article ID 949 (1990). https://doi.org/10.1088/0266-5611/6/6/006
22. McLean, W.: Strongly Elliptic Systems and Boundary Integral Equations (2000)